

TIMING CONTROL AND ALIGNMENT OF PARTICLES IN MICROCHANNEL FLOW USING DIELECTROPHORETIC FORCES

Kazuya Tatsumi, Atsushi Noma, Renato Honma, Reiko Kuriyama, Kazuyoshi Nakabe

Department of Mechanical Engineering and Science, Kyoto University, Japan

ABSTRACT

Controlling the timing, interval (spacing), and velocity of the particles and cells in microchannel flows has been an important issue to develop a high-throughput system in microfluidic devices for sensing, sorting, and encapsulating. We developed a technique that can control the timing of particles crossing a certain location in the microchannel, interval between each particle, and particle velocity for particles flowing in the microchannel by exerting forces on the particles in periodic form over time and space. In this study, we use the boxcar-type electrodes to generate the dielectrophoretic (DEP) force and control the timing of the particles and align them in the streamwise direction. Analysis based on the perturbation theory is introduced to investigate the convergence of the particle motion to the equilibrium state for the present method. We measure the particle motion in the boxcar-electrode region in the microchannel flow, and present the probability density function of the spacing (interval), velocity, and timing in relation to the applied voltage signal. The distribution demonstrates the performance of the alignment and timing control in which the variation to the target value falls in the range of several percent.

KEYWORDS: Microchannel flow, Particles, Position control, Timing control, Alignment, Focusing, Convection

1. INTRODUCTION

Controlling the position, interval (spacing), velocity, and timing of particles and cells in microchannel flows is one of the important techniques in microfluidic devices to develop a high-throughput sensing, sorting, and encapsulation systems for lab-on-a-chip and micro-total-analysis-systems. [1-2] Particles and cells mixed in fluids are supplied to the channel with the position randomly dispersed. The position of the particles and cells should be controlled to make them locate at the specific position in the channel cross-section where the sensors and sorters can perform effectively and accurately. This is called focusing of the particle and cells in the microchannel flow. Further, the spacing between the particles and cells should sufficiently be taken as several particles and cells located in the same region will incur measurement and sorting errors. Controlling the streamwise distance (interval) between the particles and cells with equal spacing (alignment) and knowing the timing when it will cross the sensor and sorting region will allow better calibration of the sensors and sorters which will result in higher accuracy. In addition to this, the alignment and timing control will also contribute significantly to the encapsulation technique. Microfluidic encapsulation generates micro-droplets sequentially in the channel and encapsulate the particles, cells, and chemical components in them. [3,4] The particles and cell should be delivered and injected to the droplets at the timing of the droplet generation with the precise number required. In the case of particles and cells supplied randomly in the channel, droplets with undesired number of particles and cells encapsulated are generated. Controlling the interval and timing, therefore, can markedly reduce the errors. From this background, controlling the timing and spacing of the particles and cells has been an essential problem and yet is a challenging issue to be solved. [5-8]

In this study, we developed a technique that can control the particle interval (spacing), velocity and the exact timing of particles crossing a certain location in the channel by applying dielectrophoretic (DEP) force to the

*Corresponding Author: tatsumi@me.kyoto-u.ac.jp

Copyright © 2019 by The Author(s). Distributed by JSME, KSME, and ASTFE with permission.

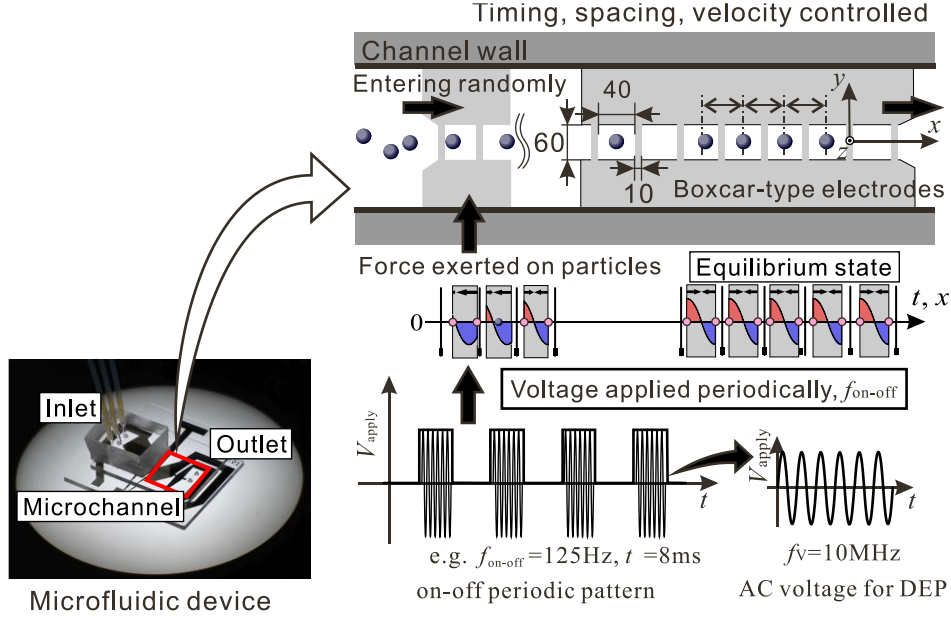


Fig. 1 Schematic of the microfluidic device and the boxcar-electrodes, and the concept of the particle alignment and timing control by applying periodic force to the particles over space and time.

particles periodically with time and space. We designed the boxcar-type electrodes to produce regions of DEP force in which particles are accelerate and decelerate periodically in the streamwise direction. The schematic of the boxcar-electrodes and the concept of the particle alignment and timing control are shown in Fig. 1. Compared to the ladder-type electrodes previously presented by the authors, [7,8] the boxcar- electrode can control the motion of the particles distributed over a wider area in the channel cross-section. It also requires less complicated process for fabrication. In this presentation, the principle of the alignment, velocity control, and the timing control of the particles is first examined based on the perturbation theory. We will then demonstrate the performance of the present technique using the boxcar- electrode by measuring the particle motion in the microchannel flow, and showing the probability density function of the deviation of the particle interval, velocity, and timing from the target value.

2. PRINCIPLE OF THE PARTICLE ALIGNMENT

To discuss the particle motion characteristic and its convergence to the equilibrium state in simplified form, we will consider a one-dimensional problem of the force distribution and particle motion. As shown in Fig. 2, the force exerted on the particle decreases linearly from positive to negative in the streamwise direction for one periodic region. The force is activated periodically for a certain period of $-\theta_0 \leq x \leq \theta_0$. We will start from the equilibrium position at which zero work will be made on the particle during one periodic cycle. We now assume that the phase of the particle against the equilibrium position is perturbed. In this case, the work applied to the particle during this cycle W_{DEP} can be written as Eq. (1), where ε and $\theta(i)$ ($i=1, 2, 3 \dots$) are the perturbation coefficient and high order terms for the order of i .

$$\begin{aligned}
 W_{DEP} &= W_{DEP,0} + \frac{\partial W_{DEP}}{\partial \theta} d\theta = W_{DEP,0} + \frac{\partial W_{DEP}}{\partial \theta} (\varepsilon \theta^{(1)} + \varepsilon^2 \theta^{(2)} + \dots) \\
 &= W_{DEP,0} - 2\theta_0 \theta^{(1)} \varepsilon - 2\theta_0 \theta^{(2)} \varepsilon^2 + \dots
 \end{aligned} \tag{1}$$

$W_{DEP,0}$ is zero and if we consider only the first order correction term, W_{DEP} is written as Eq. (2).

$$W_{DEP} \cong -2\theta_0 \theta' \tag{2}$$

We then consider the particle kinetic energy U . Having $\hat{u}_{p,0}$ be the particle average velocity in one periodic region at equilibrium state, U can be expressed as Eq. (3) with the perturbation series.

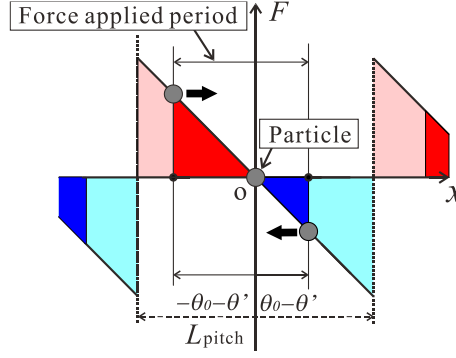


Fig. 2 Schematic of the force distribution and the force exerted on the particle when phase deviates from the equilibrium state described in a one-dimensional model.

$$U = \frac{1}{2}m\hat{u}_{p,0}^2 + \left. \frac{\partial U}{\partial \hat{u}_p} \right|_0 \hat{u}_p + \frac{1}{2} \left. \frac{\partial^2 U}{\partial \hat{u}_p^2} \right|_0 d\hat{u}_p^2 + \dots = \frac{1}{2}m\hat{u}_{p,0}^2 + m\hat{u}_{p,0} \left(\varepsilon \hat{u}_p^{(1)} + \varepsilon^2 \hat{u}_p^{(2)} + \dots \right) + \frac{1}{2}m \left(\varepsilon \hat{u}_p^{(1)} + \varepsilon^2 \hat{u}_p^{(2)} + \dots \right)^2 \quad (3)$$

Therefore, deviation from the equilibrium state ΔU can be written as $\Delta U \cong m\hat{u}_p \hat{u}_p'$, where \hat{u}_p' is the deviation from the velocity of equilibrium state $\hat{u}_{p,0}$. m is the mass of the particle.

We then define the variation of \hat{u}_p' in one periodic region as $d\hat{u}_p'$. The variation of U due to this change, which is defined here as dU , can be expressed as $dU \cong m\hat{u}_p d\hat{u}_p'$.

As dU should be equal to W_{DEP} , the following relationship can be derived.

$$d\hat{u}_p' = -\frac{2\theta_0\theta'}{m\hat{u}_0} \quad (4)$$

We will now define the variation of θ' in one periodic region as $\Delta\theta'$. $\Delta\theta'$ can be approximated as $\Delta\theta' \cong \hat{u}_p' \Delta t$, where Δt is the period of one cycle. If one periodic length is negligibly small compared with the total length of the region of interest, this can be rewritten as $\hat{u}_p' = -d\theta'/dt$. Substituting this relationship in Eq. (5), the differential equation shown as Eq. (7) can be derived.

$$\frac{d^2\theta'}{dt^2} = -\frac{2\theta_0}{m\hat{u}_{p,0}}\theta' \quad (5)$$

This gives us an oscillatory solution for θ' . As the particle will receive the drag force from the fluid, the damping term should be added to Eq. (5) which naturally gives us a solution converging to $\theta'=0$. This formula, which holds for $-\theta_0 < x < \theta_0$, is based on the condition that the flow velocity is equal to the controlled particle velocity $\hat{u}_p^* = L_{\text{pitch}}f_{\text{on-off}}$. However, this discussion can be applied also for flow velocity different from \hat{u}_p^* . In this case, the equilibrium position will move in the positive or negative direction to apply additional work on the particle so that the particle will match $\hat{u}_p^* = L_{\text{pitch}}f_{\text{on-off}}$.

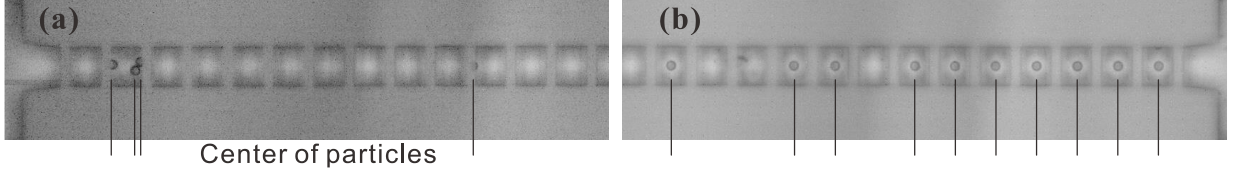
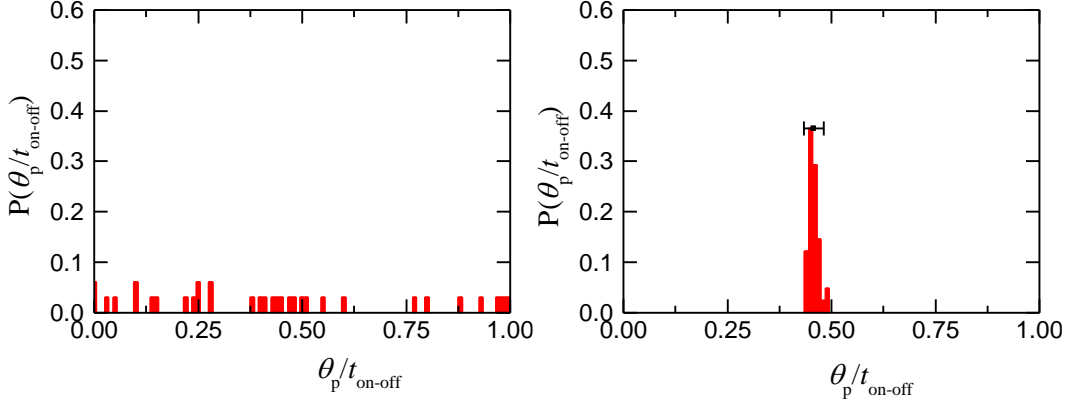
We can control the time interval between the particles and the particle velocity by changing $f_{\text{on-off}}$. The time required for the particle to move one periodic unit $L_{\text{pitch}}/\hat{u}_p$ should be same with the on-off cycle $1/f_{\text{on-off}}$. This leads to the fact that \hat{u}_p will be $L_{\text{pitch}}f_{\text{on-off}}$ and can be changed by controlling $f_{\text{on-off}}$.

3. MEASUREMENT METHODS

Boxcar-type electrodes was patterned on the channel bottom wall as shown in Fig. 1. The ground electrode was attached to the top wall covering the whole area of the top wall. The distance between parallel electrodes was 60 μm and the pitch of the crossie electrodes was 50 μm . The top and bottom walls were glass substrates on which the Pt electrodes were patterned. The layer between these substrates composing the microchannel wall was made of SU-8 (Microchem, Su-8 3050), and was fabricated through soft lithography process.

Table 1 Measurement conditions.

V_{p-p} (V)	f_V (Hz)	f_{on-off} (Hz)	U_m (mm/s)	Re
20	10M	125	7.74	0.54

**Fig. 3** Snapshots of the particles at the inlet and outlet of the boxcar-electrode.**Fig. 4** Probability density function for time difference between particles located at the middle of the boxcar-electrode region and the signal rise of the applied voltage: measured at inlet (left) and outlet (right).

The channel height is 42 μm and width is 200 μm at the boxcar-electrode region. Fluid was supplied to the inlets of the channel by a pump driven by pressurized air. Particles flowing from the center channel were focused and guided to the inlet of the boxcar-electrode region by rail-type electrodes, which were placed in the upstream of the boxcar-electrode region. The details of the structure and function of the microchannel flow and rail-electrode are presented in the authors' previous works [7,8].

Polystyrene micro particles of 12 μm diameters (Thermoscientific Co., 4212A) were used. The working fluid was water (Milli-Q water) to which sodium lauryl sulfate (SLS) was mixed with 0.1wt%. The motion of the particles was recorded by a high speed video camera and microscope. The frame rate and resolution of the measurement were 10,000fps and 0.88 μm , respectively. We applied alternate current voltage to the electrode using a function generator with peak-to-peak voltage of $V_{p-p}=20\text{V}$ and frequency of $f_V=10\text{MHz}$. This voltage was turned on and off periodically with frequency of $f_{on-off}=125\text{Hz}$. The particle position and velocity in the channel was obtained from the series of images by motion analysis software (Library Co. Ltd., Move-tr/2D ver. 7.90). Table 1 shows the representative experimental conditions. The characteristic length and velocity of the Reynolds number are the channel hydraulic diameter and the cross-sectional average velocity.

4. RESULTS AND DISCUSSION

Figure 3 shows the snapshots of the particles flowing over the boxcar-electrode at the inlet and outlet regions, respectively. In Fig. 3 (a), the particles are entering the region with random spacing, and some particles form groups (clusters) having the spanwise position not fully focused. On the other hand, in Fig. 3 (b), clusters are not observed and the particles are focused at the centerline accurately. Moreover, the particles are equally spaced in the streamwise direction with distance equal to the pitch of the boxcar-electrodes, L_{pitch} , or its multiples. Although not shown here but will in the presentation, the probability density function of the interval between the particles showed a peak distribution with 95% confidence interval falling inside the range of $\pm 1.9\%$ of $t_{on-off} = 1/f_{on-off}$. Furthermore, the probability density function of the particle velocity showed a maximum peak at the value equal to $L_{pitch}f_{on-off}$, and the deviation was $\pm 2.6\%$ with the 95% confidence interval.

The relative position to the traverse electrodes are the same for all particles shown in Fig. 3 (b). This characteristics having identical relative position to the electrode was same for other time (phases). This implies that if the particle motion and the voltage signal applied to the electrode are synchronized, we can predict and control the timing of the particles passing a specific streamwise position from/with the voltage signal. To evaluate the capability of the timing control using the present technique, we measured the particle motion with synchronizing the camera recording with the voltage signal. The time difference between the signal rise of the voltage and the time when the particles crosses the middle of the boxcar-electrode region ($x/L_{\text{pitch}}=0.5$) is defined as θ_p [s]. The probability density function (PDF) of $\theta_p/t_{\text{on-off}}$ is shown in Fig. 4. At the inlet of the boxcar-electrode, the PDF of $\theta_p/t_{\text{on-off}}$ shows a uniform distribution indicating that the timing in relation to the applied voltage is random. On the other hand, the PDF of $\theta_p/t_{\text{on-off}}$ shows a maximum peak at $\theta_p/t_{\text{on-off}}=0.46$ with the 95% confidence interval falling inside the range of $\pm 2.5\%$. This represents the fact that we can predict the exact timing when the particle passes a certain position from the applied voltage signal within this accuracy. Further, if a specific timing is required for the particles, e.g. the timing when the particle should cross the sensor region or enter the droplet, we can match the timing by adjusting the phase of the voltage signal.

As mentioned previously, the PDF of the time interval and velocity will be discussed in the presentation. Further, the relationship between the phase deviation from the equilibrium state and the particle velocity is measured and will be shown to verify the analytical results and evaluate the particle motion characteristics: how the force is exerted on the particles and how the particles move as they converge to the equilibrium state.

5. CONCLUSIONS

Timing, interval (spacing), and velocity of the particles flowing in the microchannel was controlled by exerting dielectrophoretic forces on the particles in periodic form over space and time using boxcar-type electrodes. The analytical results showed that the present method can control the particle position to the equilibrium position at which the interval (spacing) and the velocity of particles are equal to the cycle (pitch) of the periodicity $1/f_{\text{on-off}}$ (L_{pitch}) and $L_{\text{pitch}}f_{\text{on-off}}$. The measured probability density distribution for the deviation of the timing, spacing (interval), and velocity from the target value showed that the values can be controlled within the accuracy of $\pm 2.5\%$, $\pm 1.9\%$, and 2.6% , respectively. Although not shown here but will in the presentation, the numerical results and the measurement for the phase deviation from the equilibrium state of the particles showed that the particles with larger/smaller spacing (interval) or velocity compared with the target value will give a phase shift leading to additional acceleration and deceleration of the particle motion. This agreed well with the analytical results.

ACKNOWLEDGMENTS

This work was supported by the Japan Society for the Promotion of Science KAKENHI Grant Number 17K18841, and partially by Micro/Nano Fabrication Hub in Kyoto University of "Low-Carbon Research Network" funded by the Ministry of Education, Culture, Sports, Science and Technology (MEXT), Japan.

REFERENCES

- [1] Sun, T., Green, N.G., Gawad, S., Morgan, H., "Analytical electric field and sensitivity analysis for two microfluidic impedance cytometer designs", *IET Nanobiotechnol.*, **1**, 69–79 (2007).
- [2] Riordon, J., Nash, M., Calderini, M., Godin, M., "Using active microfluidic flow focusing to sort particles and cells based on high-resolution volume measurements", *Microelectronic Engineering*, **118**, 35-40 (2014).
- [3] Abate, A. R., Chen, C-H., Agresti, J. J., Weitz, D. A., "Beating Poisson encapsulation statistics using close-packed ordering", *Lab Chip*, **9**, 2628-2631 (2009).
- [4] Mazutis, L., Gilbert, J., Lloyd, U., Weitz, D. A., Griffiths, A. D., Heyman, J. A., "Single-cell analysis and sorting using droplet-based microfluidics", *Nature Protocols*, **8**, 870-891 (2013).
- [5] Laurell, T., Petersson, F., Nilsson, A., "Chip integrated strategies for acoustic separation and manipulation of cells and particles", *Chem. Soc. Rev.*, **36**, 492–506 (2007).
- [6] Chung, A. J., Gossett, D. R., Di Carlo, D., "Three dimensional, sheathless, and high-throughput microparticle inertial focusing through geometry-induced secondary flows", *Small*, **9**, 685-690 (2013).
- [7] Tatsumi, K., Kawano, K., Okui, H., Shintani, H., Nakabe, K., "Analysis and measurement of dielectrophoretic manipulation of particles and lymphocytes using rail-type electrodes," *Medical Engineering and Physics*, **38**, 24-32 (2016).
- [8] Tatsumi, K., Kawano, K., Shintani, H., Nakabe, K., "Particle timing control and alignment in microchannel flow by applying periodic force control using dielectrophoretic force", *Analytical Chemistry*, **91** (10), 6462-6470 (2019).